

Spin and Orbital States and Their Phase Transitions of the Perovskite-Type Ti Oxides: Weak Coupling Approach

Masahito MOCHIZUKI

*Institute for Solid State Physics, University of Tokyo,
5-1-5 Kashiwa-no-ha, Kashiwa, Chiba 277-8581*

(Received October 26, 2018)

The magnetic phase diagram of the perovskite-type Ti oxides as a function of the GdFeO₃-type distortion is examined by using the Hartree-Fock analysis of a multiband d - p Hamiltonian from a viewpoint of competitions of the spin-orbit interaction, the Jahn-Teller (JT) level-splitting and spin-orbital superexchange interactions. Near the antiferromagnetic (AFM)-to-ferromagnetic (FM) phase boundary, A-type AFM [AFM(A)] and FM states accompanied by a certain type of orbital ordering are lowered in energy at large JT distortion, which is in agreement with the previous strong coupling study. With increasing the GdFeO₃-type distortion, their phase transition occurs. Through this magnetic phase transition, the orbital state hardly changes, which induces nearly continuous change in the spin coupling along the c -axis from negative to positive. The resultant strong two-dimensionality in the spin coupling near the phase boundary is attributed to the strong suppression of T_N and T_C , which is experimentally observed. On the other hand, at small GdFeO₃-type without JT distortions, which correspond to LaTiO₃, the most stable solution is not G-type AFM [AFM(G)] but FM. Although the spin-orbit interaction has been considered to be relevant at the small or no JT distortion of LaTiO₃ in the literature, our analysis indicates that the spin-orbit interaction is irrelevant to the AFM(G) state in LaTiO₃ and superexchange-type interaction dominates. On the basis of further investigations on the nature of this FM state and other solutions, this discrepancy is discussed in detail.

KEYWORDS: perovskite-type Ti oxides, GdFeO₃-type distortion, d -level degeneracy, d -type Jahn-Teller distortion, spin-orbit interaction, multiband d - p model

§1. Introduction

In transition-metal oxides, strong electron correlations often localize the $3d$ electrons and the system becomes an insulator (a Mott insulator).¹⁾ These compounds have recently attracted considerable interest since they show rich magnetic and orbital phases. In particular, perovskite-type oxides $RM\text{O}_3$, where R denotes a trivalent rare-earth ion (i.e., La, Pr, Nd, ..., Y) and M is a transition-metal ion (i.e., Ti, V, ..., Ni, Cu) exhibit a variety of magnetic and electronic properties caused by an interplay of charge, spin and orbital degrees of freedom.

The perovskite-type Ti oxide $RTi\text{O}_3$ is a prototypical example. In these compounds, Ti^{3+} has a t_{2g}^1 configuration, and one of the threefold t_{2g} -orbitals is occupied at each transition-metal site. They have attracted much interest since these systems show various magnetic and orbital orderings owing to the threefold degeneracy of the t_{2g} orbitals. It requires to take both spin and orbital fluctuations into consideration to explain competitions of such rich phases. Moreover, the spin-orbit interaction would make the magnetic and orbital structures more complicated since the t_{2g} orbitals are strongly affected by the interaction.

The crystal structure of $RTi\text{O}_6$ is an orthorhombically distorted cubic-perovskite (GdFeO₃-type distortion) in which the TiO_6 octahedra forming the perovskite lattice tilt alternately as shown in Fig. 1. The magnitude of the distortion depends on the ionic radii of the R ions. With a small ionic radius of the R ion, the

lattice structure is more distorted and the bond angle is more significantly decreased from 180°. In LaTiO₃, the bond angle is 157° (ab -plane) and 156° (c -axis), but 144° (ab -plane) and 140° (c -axis) in YTiO₃.²⁾ The distortion can be controlled by the use of the solid-solution systems $\text{La}_{1-y}\text{Y}_y\text{TiO}_3$ or in $RTi\text{O}_3$, by varying the R ions. In particular, by varying the Y concentration in $\text{La}_{1-y}\text{Y}_y\text{TiO}_3$, we can control the bond angle almost continuously from 157° ($y = 0$) to 140° ($y = 1$).

In YTiO₃, a d -type JT distortion has been observed in which the longer and shorter Ti-O bond lengths are ~ 2.08 Å and ~ 2.02 Å, respectively.³⁾ In the d -type JT distortion, the xy and yz orbitals are stabilized at sites 1 and 3, and the xy and zx orbitals are stabilized at sites 2 and 4. On the other hand, LaTiO₃ exhibits no detectable JT distortion.

Recently, the magnetic phase diagrams have been studied as functions of the magnitude of GdFeO₃-type distortion.⁴⁻⁷⁾ In La-rich ($y < 0.6$) systems or in the compounds with large R ions, in which the GdFeO₃-type distortion is relatively small, an AFM ground state is realized. In particular, LaTiO₃ exhibits a AFM(G) ground state with magnetic moment of $0.45 \mu_B$, which is strongly reduced from spin-only moment, and the Néel temperature (T_N) is about 130 K. With increasing the Y concentration or varying the R site with smaller-sized ions (an increase of the GdFeO₃-type distortion), T_N decreases rapidly and is suppressed to almost zero, subsequently a FM ordering appears. In Y-rich systems and in YTiO₃

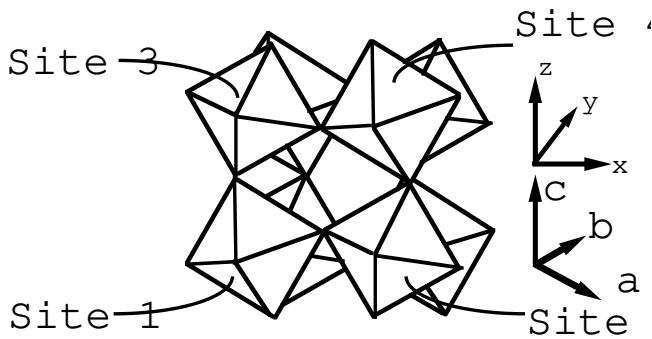


Fig. 1. GdFeO₃-type distortion.

in which the GdFeO₃-type distortion is relatively large, the system shows a FM ground state.

In order to elucidate these phase diagrams, model Hartree-Fock studies have been done previously.^{8,9)} In these weak coupling studies, it is claimed that in LaTiO₃ with small GdFeO₃-type distortion, a AFM(G) state with the spin-orbit ground state is realized for the small or no JT distortion, and resultant unquenched orbital moment is considered to be consistent with the strong reduction of the moment. On the other hand, a FM state accompanied by an orbital ordering is realized in YTiO₃ with large JT distortion. However, in these studies, the nature of the phase diagrams has not been elucidated sufficiently in the following sense. At first sight, we can expect the first-order transition between completely different symmetry breaking in which T_N and T_C remain nonzero at the AFM-FM phase boundary. However, in the magnetic phase diagrams, T_N and T_C are strongly suppressed around the phase boundary. This strong suppression implies a continuous-type transition at $T = 0$ and contradicts our naive expectation. This second-order like phase transition is not explained in these studies, and has been an issue of interest.

Recently, in order to clarify this problem, effective Hamiltonian in the insulating limit has been applied to this system.^{10,11)} According to these strong coupling studies, in the AFM phase near the AFM-FM phase boundary, an AFM(A) ground state is realized. This AFM(A) phase has not been studied in the previous weak coupling approach. Moreover, since the orbital state is strongly stabilized and changes only little through the transition, strong two-dimensionality in spin-coupling is predicted near the phase boundary and the strong suppressions of T_N and T_C are naturally understood. In these studies, a large JT distortion is assumed in order to focus on the situation near the AFM-FM phase boundary, and the spin-orbit interaction is neglected on the basis of the large energy-splitting due to the JT distortion. In addition, the AFM(G) state in LaTiO₃ with small or no JT distortion has not been reproduced.

However, the spin-orbit interaction may become relevant in the systems with small or no JT distortion such as LaTiO₃. While the spin-orbit interaction can be neglected if the JT distortion is large, we can expect a strong competition between the spin-orbit interaction

and JT level-splitting with decreasing the JT distortion. With sufficiently small JT distortion, the system may well be described by the spin-orbit ground state. Besides, successive spin-orbital superexchange interactions may dominate over the spin-orbit interaction even without JT distortion. At this stage, it is an issue of importance to examine the phase diagrams from a viewpoint of their competitions. In the weak coupling approach in which transfers of electrons and spin-orbit interaction are treated in a non-perturbative manner, we can consider both effects on an equal footing. This approach is appropriate for a systematic study on the interplay of them. In these senses, the weak-coupling and the strong-coupling studies are complementary to each other, and analysis from the weak coupling approach is important.

In this paper, we investigate the magnetic phase diagrams by using the Hartree-Fock analysis of the multi-band $d-p$ Hamiltonian. We study the magnetic and orbital states as functions of the GdFeO₃-type and d -type JT distortions. Since effects of both electron transfers and spin-orbit interaction are taken into account on an equal footing, this model is appropriate for a study on the competitions of spin-orbit interaction, JT level-splitting and superexchange interactions. The weak coupling treatment does not properly reproduce the energy scale of the superexchange interaction J defined in the strong coupling region, where J is proportional to t^2/U with t and U being typical transfer and on-site Coulomb repulsion. However, the physics contained in the reproduction of the superexchange interaction with AFM and/or antiferro-orbital (AF-orbital) is expected to be adiabatically connected with the SDW type symmetry breaking in the weak-coupling Hartree-Fock solution. Therefore, we will refer the stabilization of the SDW (or orbital density wave) type solution with AFM (or AF-orbital) symmetry breaking to the superexchange mechanism.

Pioneering works by using this method have already been done by Mizokawa and Fujimori.^{8,9)} However, concerning the region of small GdFeO₃-type distortion, we have come to a different conclusion by studying orbital-spin states which they have overlooked. We show that in the small GdFeO₃-type distortion without JT level-splitting, a FM spin state accompanied by an AF-orbital ordering is stabilized by the energy gains of both spin-orbit and superexchange interactions. In this FM solution, the spin-orbit ground state is not realized at certain sites, which suggests that the spin-orbital superexchange interactions due to the electron transfers dominate over the spin-orbit interaction even without JT distortion. In the previous studies, AFM(G) state with spin-orbit ground state has been claimed to be stabilized without JT distortion. However, in these studies, the stabilization of this AFM(G) state is concluded only from comparison of the energies between this AFM(G) solution and a FM solution with higher energy, and our FM solution is ignored. Our FM state has not been reproduced so far, and is studied for the first time by our weak coupling approach. We conclude that the AFM(G) state in LaTiO₃ does not accompany with spin-orbit ground state, and there exists another origin for its emergence.

Recent neutron-scattering experiment shows the spin-wave spectrum of LaTiO₃ well described by a spin-1/2 isotropic Heisenberg model on the cubic lattice, and absence of unquenched orbital momentum.¹²⁾ This result also seems to contradict the naive prediction of spin-orbit ground state with no JT distortion. By studying a model including the spin-orbit interaction, we propose some statements on this experimental result.

Moreover, we apply this method to the systems near the AFM-FM phase boundary for the first time. We show that the strange behavior of the magnetic phase transition is well described on the basis of JT ground state when we consider the experimentally observed large JT distortion. The results on the properties and nature of the phase transition are in agreement with those obtained by the previous strong coupling approaches, which indicates its validity irrespective of the coupling strength.^{10, 11)} In addition, we study a magnetic and orbital phase diagram in the plane of the GdFeO₃-type and *d*-type JT distortions in order to examine how extent the physics of AFM-FM phase transition in strong coupling limit survives when the JT level-splitting competes with the spin-orbit interaction.

The organization of this paper is as follows. In § 2, we introduce the multiband *d-p* Hamiltonian to describe the realistic systems of the perovskite-type Ti oxides. In § 3, numerical results calculated by applying the unrestricted Hartree-Fock approximation are presented. Section. 4 is devoted to the summary and conclusions.

§2. Multiband *d-p* model

We employ the following Hamiltonian:

$$H^{dp} = H_{d0} + H_p + H_{tdp} + H_{tpp} + H_h + H_{\text{on-site}}, \quad (1)$$

with

$$H_{d0} = \sum_{\alpha, i, \gamma, \sigma} \varepsilon_d^0 d_{\alpha, i\gamma\sigma}^\dagger d_{\alpha, i\gamma\sigma}, \quad (2)$$

$$H_p = \sum_{\alpha, j, l, \sigma} \varepsilon_p p_{\alpha, jl\sigma}^\dagger p_{\alpha, jl\sigma}, \quad (3)$$

$$H_{tdp} = \sum_{\alpha, i, \gamma, \alpha', j, l, \sigma} t_{\alpha i\gamma, \alpha' j l}^{dp} d_{\alpha, i\gamma\sigma}^\dagger p_{\alpha', j l\sigma} + \text{h.c.}, \quad (4)$$

$$H_{tpp} = \sum_{\alpha, j, l, \alpha', j', l', \sigma} t_{\alpha j l, \alpha' j' l'}^{pp} p_{\alpha, j l\sigma}^\dagger p_{\alpha', j' l'\sigma} + \text{h.c.}, \quad (5)$$

$$H_h = \sum_{\alpha, i, \gamma, \gamma', \sigma, \sigma'} h_{\gamma\sigma, \gamma'\sigma'} d_{\alpha, i\gamma\sigma}^\dagger d_{\alpha, i\gamma'\sigma'}, \quad (6)$$

$$H_{\text{on-site}} = H_u + H_{u'} + H_j + H_{j'}, \quad (7)$$

where $d_{\alpha, i\gamma\sigma}^\dagger$ is a creation operator of an electron with spin $\sigma (= \uparrow, \downarrow)$ in the $3d$ orbital γ at Ti site i in the α -th unit cell, and $p_{\alpha, jl\sigma}^\dagger$ is a creation operator of an electron with spin $\sigma (= \uparrow, \downarrow)$ in the $2p$ orbital l at oxygen site j in the α -th unit cell. Here, H_{d0} and H_p stand for the bare level energies of Ti $3d$ and O $2p$ orbitals, respectively. H_{tdp} and H_{tpp} are *d-p* and *p-p* hybridization terms, respectively. H_h denotes the crystal field and spin-orbit interaction represented by the parameter $\xi = 0.018$ eV.¹³⁾ The term $H_{\text{on-site}}$ represents on-site *d-d* Coulomb in-

teractions. $t_{\alpha i\gamma, \alpha' j l}^{dp}$ and $t_{\alpha j l, \alpha' j' l'}^{pp}$ are nearest-neighbor *d-p* and *p-p* transfers, respectively, which are given in terms of Slater-Koster parameters $V_{pd\pi}$, $V_{pd\sigma}$, $V_{pp\pi}$ and $V_{pp\sigma}$.¹⁴⁾ $H_{\text{on-site}}$ term consists of the following four contributions:

$$H_u = \sum_{\alpha, i, \gamma} u d_{\alpha, i\gamma\uparrow}^\dagger d_{\alpha, i\gamma\uparrow} d_{\alpha, i\gamma\downarrow}^\dagger d_{\alpha, i\gamma\downarrow}, \quad (8)$$

$$H_{u'} = \sum_{\alpha, i, \gamma > \gamma', \sigma, \sigma'} u' d_{\alpha, i\gamma\sigma}^\dagger d_{\alpha, i\gamma\sigma} d_{\alpha, i\gamma'\sigma'}^\dagger d_{\alpha, i\gamma'\sigma'}, \quad (9)$$

$$H_j = \sum_{\alpha, i, \gamma > \gamma', \sigma, \sigma'} j d_{\alpha, i\gamma\sigma}^\dagger d_{\alpha, i\gamma\sigma} d_{\alpha, i\gamma'\sigma'}^\dagger d_{\alpha, i\gamma'\sigma'}, \quad (10)$$

$$H_{j'} = \sum_{\alpha, i, \gamma \neq \gamma'} j' d_{\alpha, i\gamma\uparrow}^\dagger d_{\alpha, i\gamma\uparrow} d_{\alpha, i\gamma\downarrow}^\dagger d_{\alpha, i\gamma\downarrow}, \quad (11)$$

where H_u and $H_{u'}$ are the intra- and inter-orbital Coulomb interactions and H_j and $H_{j'}$ denote the exchange interactions. The term H_j is the origin of the Hund's rule coupling which strongly favors the spin alignment in the same direction on the same atoms. These interactions are expressed by Kanamori parameters, u , u' , j and j' which satisfy the following relations:^{15, 16)}

$$u = U + \frac{20}{9}j, \quad (12)$$

$$u' = u - 2j, \quad (13)$$

$$j = j'. \quad (14)$$

Here, U gives the magnitude of the multiplet-averaged *d-d* Coulomb interaction. The charge-transfer energy Δ , which describes the energy difference between occupied O $2p$ and unoccupied Ti $3d$ orbitals, is defined by U and energies of the bare Ti $3d$ and O $2p$ orbitals ε_d^0 and ε_p as follows,

$$\Delta = \varepsilon_d^0 + U - \varepsilon_p. \quad (15)$$

The values of Δ , U and $V_{pd\sigma}$ are estimated by the cluster-model analyses of valence-band and transition-metal $2p$ core-level photoemission spectra.^{17, 18)} We take the values of these parameters as $\Delta = 7.0$ eV, $U = 4.0$ eV, $V_{pd\sigma} = -2.2$ eV and $j = 0.64$ eV throughout the present calculation. The ratio $V_{pd\sigma}/V_{pd\pi}$ is fixed at -2.18 , and $V_{pp\sigma}$ and $V_{pp\pi}$ at 0.60 eV and -0.15 eV, respectively¹⁹⁻²¹⁾. The effects of the GdFeO₃-type distortion and the *d*-type JT distortion are reflected on the hopping integrals. The GdFeO₃-type structure is orthorhombic with orthogonal *a*-, *b*- and *c*-axes which can be obtained by rotating the four octahedra in the unit cell. Let us represent the four octahedra in the unit cell as site 1, site 2, site 3 and site 4 as shown in Fig. 1. Here, we simulate the GdFeO₃-type structure by tilting the TiO₆ octahedra by $+\theta$ and $-\theta$ about the $(1, 1, 1)$ and $(-1, -1, 1)$ axes with respect to the *x, y* and *z* axes. The magnitude of the GdFeO₃-type distortion is expressed by the bond angle. The magnitude of the JT distortion can be denoted by the ratio $[V_{pd\sigma}^s/V_{pd\sigma}^l]^{1/3}$; here, $V_{pd\sigma}^s$ and $V_{pd\sigma}^l$ are the transfer integrals for the shorter and longer Ti-O bonds, respectively. The value for YTiO₃ estimated by using Harrison's rule takes ~ 1.040 ¹⁹⁾. This large JT distortion is also considered to be realized near the AFM-FM phase

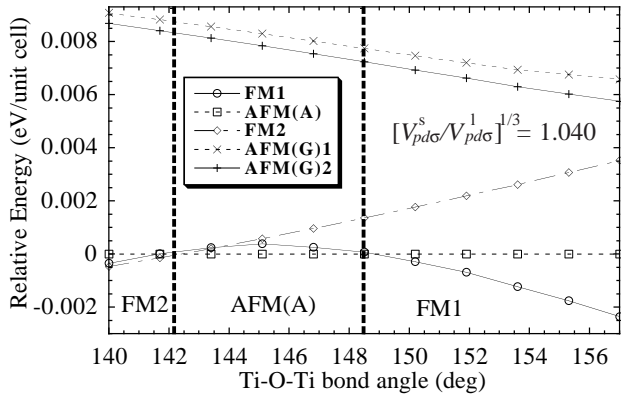


Fig. 2. Energies of various spin and orbital configurations relative to that of AFM(A) state as functions of the Ti-O-Ti bond angle in the case of $[V_{pd\sigma}^s/V_{pd\sigma}^l]^{1/3} = 1.040$.

boundary.

We can rewrite the Hamiltonian in the k -space form by using the following Bloch-electron operators,

$$d_{\mathbf{k},i\gamma\sigma}^\dagger = \frac{1}{\sqrt{N}} \sum_{\alpha} e^{i\mathbf{k}\cdot\mathbf{R}_{\alpha}} d_{\alpha,i\gamma\sigma}^\dagger, \quad (16)$$

$$p_{\mathbf{k},j\ell\sigma}^\dagger = \frac{1}{\sqrt{N}} \sum_{\alpha} e^{i\mathbf{k}\cdot\mathbf{R}_{\alpha}} p_{\alpha,j\ell\sigma}^\dagger, \quad (17)$$

where \mathbf{k} labels the wave vector in the first Brillouin zone.

§3. Results and Discussions

In this section, we present the numerical results calculated by applying the unrestricted Hartree-Fock approximation to the multiband d - p model introduced in the previous section. In our calculations, we have concentrated on uniform solutions. At this stage, the order parameters can be written as,

$$\langle d_{\alpha,i\gamma\sigma}^\dagger d_{\alpha,i\gamma'\sigma'} \rangle = \frac{1}{N} \sum_{\mathbf{k}} \langle d_{\mathbf{k},i\gamma\sigma}^\dagger d_{\mathbf{k},i\gamma'\sigma'} \rangle \quad (18)$$

which are to be determined self-consistently. We have taken 512 \mathbf{k} points in the first Brillouin zone of the GdFeO₃-type structure and iterated the self-consistency cycle until the convergence of all the order parameters within errors of 1×10^{-4} . It should be noted that the basis of the Ti 3d orbitals are defined by using x -, y -, and z -axes attached to each TiO₆ octahedron in this paper.

First, in order to focus on the situation near the AFM-FM phase boundary, the magnitude of the JT distortion: $[V_{pd\sigma}^s/V_{pd\sigma}^l]^{1/3}$ is fixed at 1.040, which is considered to be realized around the AFM-FM phase boundary.

In Fig. 2, relative energies of various spin and orbital configurations are plotted as functions of the Ti-O-Ti bond angle from 157° to 140°. In the small GdFeO₃-type distortion, a FM solution with (yz, xy, xy, zx) -type orbital ordering in which site 1, 2, 3 and 4 are dominantly occupied by yz , xy , xy and zx , respectively (FM1 solution) is stabilized (see Fig. 3) since the FM state with the orbital configuration in which the neighboring occupied-orbitals are approximately orthogonal (AF-orbital ordering) is favored both by transfers and by the exchange

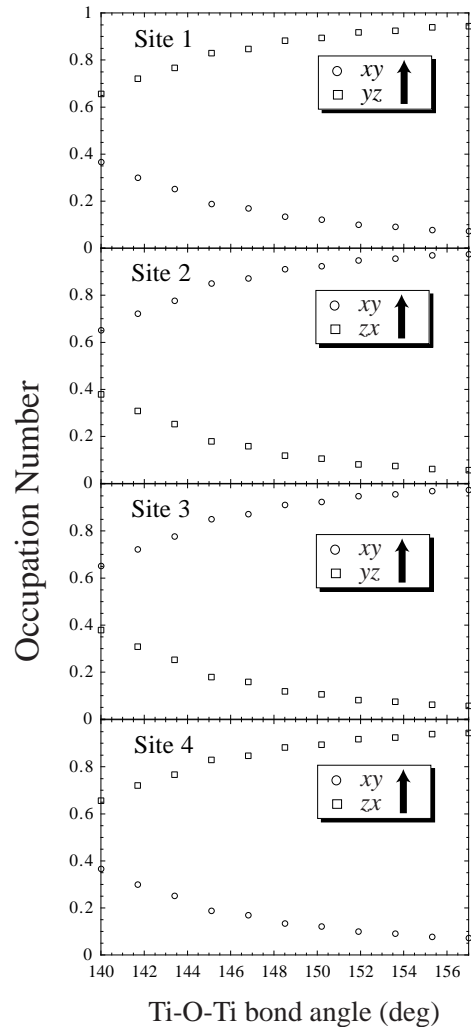


Fig. 3. The orbital occupation in the majority spin states of FM1 state as a function of the Ti-O-Ti bond angle in the case of $[V_{pd\sigma}^s/V_{pd\sigma}^l]^{1/3} = 1.040$.

interaction j . A AFM(G) solution with (yz, xy, xy, zx) -type orbital ordering [AFM(G)1] has much higher energy. However, it should be noted that the present calculations are carried out in the case of large JT distortion so that the obtained FM1 solution with the small GdFeO₃-type distortion does not necessarily contradict the emergence of AFM(G)-ground state in LaTiO₃ with no JT distortion.

As the GdFeO₃-type distortion increases, the (yz, xy, xy, zx) -type orbital state becomes unstable. Instead, the solutions with the orbital state in which xy orbital is mixed into the occupied yz and zx orbitals [(yz, zx, yz, zx) -type orbital state] become stable (see Fig. 4). By moderately increasing the distortion, AFM(A) state with (yz, zx, yz, zx) -type orbital ordering is stabilized relative to FM1 solution. With further decreasing of the bond angle, the FM state with (yz, zx, yz, zx) -type orbital ordering (FM2 solution) is stabilized. The AFM(G) solution with (yz, zx, yz, zx) -type orbital ordering [AFM(G)2] has much higher energy relative to the other solutions. The AFM(A) to FM2 phase transition occurs at $\angle\text{Ti-O-Ti} \sim 142^\circ$. These

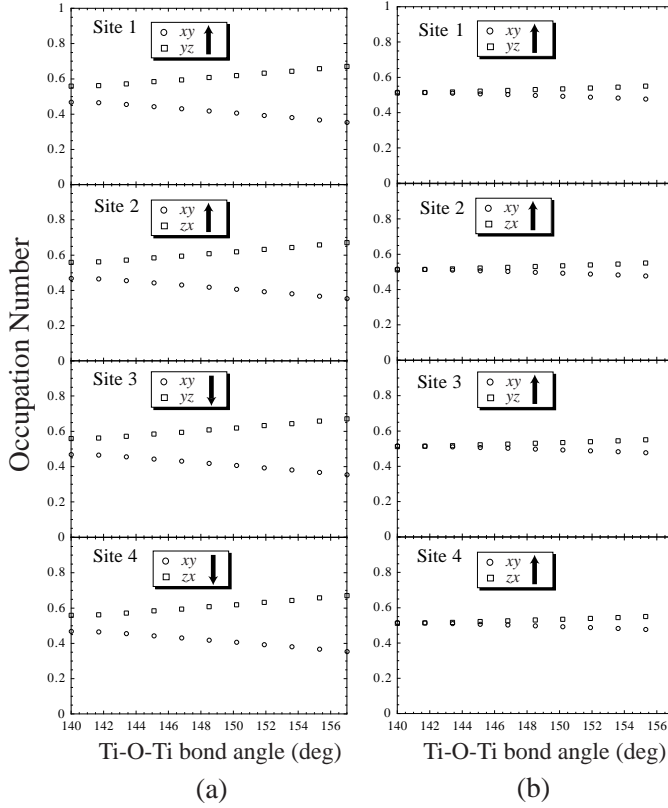


Fig. 4. The orbital occupation in the majority spin states of (a) AFM(A) and (b) FM2 states as functions of the Ti-O-Ti bond angle in the case of $[V_{pd\sigma}^s/V_{pd\sigma}^l]^{1/3} = 1.040$.

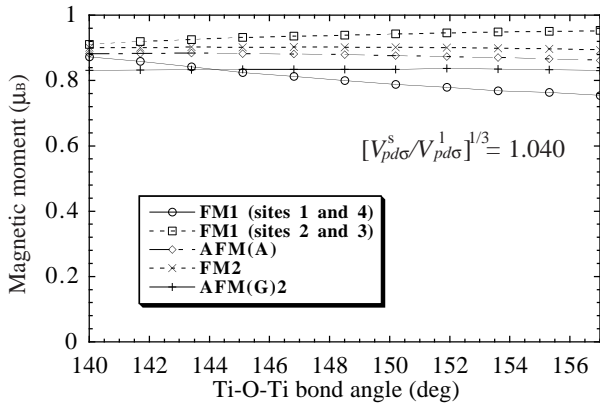


Fig. 5. Magnetic moment of various spin and orbital states as functions of the Ti-O-Ti bond angle in the case of $[V_{pd\sigma}^s/V_{pd\sigma}^l]^{1/3} = 1.040$. In the FM1 state, the magnitude of the magnetic moment is different between sites 1, 4 and sites 2, 3.

AFM(A) and FM2 states are expected to be realized in the systems which are located near the AFM-FM phase boundary. In addition, we note that in the large JT distortion of 1.040, the spin-orbit ground state does not have any stable solutions.

In Fig. 5, we have plotted the magnetic moment of the various spin and orbital solutions as functions of the

Ti-O-Ti bond angle. With this large JT distortion, the orbital angular momentum is mostly quenched and the magnetic moment basically consists of the spin-only moment. This indicates that the effect of the spin-orbit interaction can be neglected and the system near the phase boundary is well described by the JT ground state.

Under this large d -type JT distortion, the occupation of the higher t_{2g} orbitals at sites 1, 2, 3 and 4 are close to zero so that the occupied orbitals at each site can be expressed by the linear combination of the twofold degenerate lowered orbitals, approximately. In addition, since the order of the indirect d - d -transfers mediated by the O $2p$ orbitals is $\frac{V_{pd\pi}^2}{\Delta} \sim 0.2$ eV and sufficiently small compared with U , the \mathbf{k} -dependence of the coefficients for the linear combinations can be neglected. So that, we can express the occupied orbitals at i -th site by the coefficients $C_{\alpha,i\gamma\sigma}$ as,

$$\sum_{\gamma}' C_{\alpha,i\gamma\sigma} |\gamma\rangle. \quad (19)$$

Here, \sum_{γ}' denotes the summation over the twofold lowered orbitals in the d -type JT distortion at i -th site, namely, xy and yz orbitals at sites 1 and 3, and xy and zx orbitals at sites 2 and 4. Since the spin-orbit interaction is not effective under the large JT distortion, the imaginary parts of the coefficients are negligible. At this stage, we define the absolute values of the coefficients in the normalized form as,

$$|C_{\alpha,i\gamma\sigma}| = \sqrt{\frac{\langle d_{\alpha,i\gamma\sigma}^{\dagger} d_{\alpha,i\gamma\sigma} \rangle}{\sum_{\gamma'} \langle d_{\alpha,i\gamma'\sigma}^{\dagger} d_{\alpha,i\gamma'\sigma} \rangle}}. \quad (20)$$

The orbital states realized in the AFM(A), AFM(G)2 and FM2 solutions can be specified by using angles $\theta_{\text{AFM(A)}}$, $\theta_{\text{AFM(G)2}}$ and θ_{FM} as,

$$\begin{aligned} \text{site 1; } & \cos\theta_x |xy\rangle + \sin\theta_x |yz\rangle, \\ \text{site 2; } & \cos\theta_x |xy\rangle + \sin\theta_x |zx\rangle, \\ \text{site 3; } & -\cos\theta_x |xy\rangle + \sin\theta_x |yz\rangle, \\ \text{site 4; } & -\cos\theta_x |xy\rangle + \sin\theta_x |zx\rangle, \end{aligned} \quad (21)$$

where $x = \text{AFM(A)}$, AFM(G)2 and FM2 . In Fig. 6, the angles for the AFM(A), AFM(G)2 and FM2 solutions are plotted as functions of the Ti-O-Ti bond angle. In AFM(A) state, the sites 1, 2, 3 and 4 are occupied by $c_1 yz + c_2 xy$, $c_1 zx + c_2 xy$, $c_1 yz - c_2 xy$ and $c_1 zx - c_2 xy$ ($c_1^2 + c_2^2 = 1$), respectively. In particular, the difference between c_1 and c_2 tends to be small with increasing the GdFeO₃-type distortion, and both c_1 and c_2 take approximately $1/\sqrt{2}$ for the large distortion. Moreover, the similar orbital state is also realized in FM2 state, and both c_1 and c_2 also take approximately $1/\sqrt{2}$. This orbital state is in agreement with previous theoretical predictions,^{9, 11, 22, 23}) and is observed experimentally in YTiO₃.²⁴⁻²⁷) The difference between $\theta_{\text{AFM(A)}}$ and θ_{FM2} is very small, especially in the largely distorted region or near the AFM(A)-FM2 phase boundary. This indicates that the orbital ordering hardly changes through the magnetic phase transition. Then, the AFM(A)-to-FM2

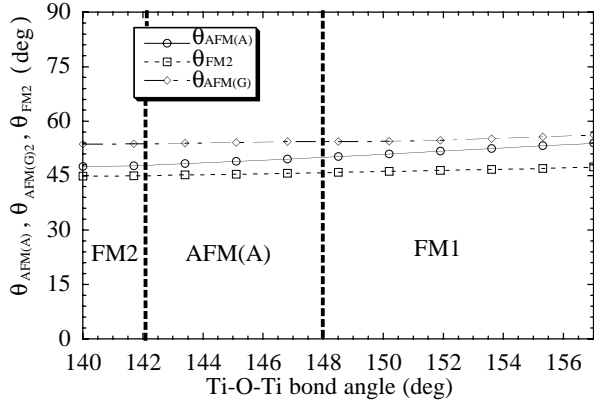


Fig. 6. The orbital structures in AFM(A), AFM(G)2 and FM2 solutions as functions of the Ti-O-Ti bond angle. The difference between those of AFM(A) and FM2 is considerably small, particularly for the large GdFeO₃-type distortion or near the AFM(A)-FM2 phase boundary.

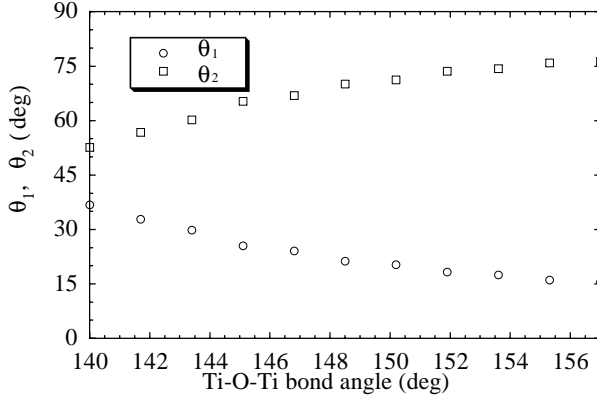


Fig. 7. The orbital structure in the FM1 solution as a function of the Ti-O-Ti bond angle. In the small GdFeO₃-type distortion, an almost complete (yz, xy, xy, zx)-type orbital ordering is realized.

phase transition is identified as a nearly continuous one with a tiny jump in the spin-exchange interaction along the c -axis from positive to negative and it takes approximately zero at the phase boundary. On the contrary, the FM spin-exchange interaction is constantly realized in the ab -plane. The resultant strong two-dimensionality in the spin coupling can cause the strong suppression of T_N and T_C near the phase boundary. These are all in agreement with the previous strong coupling studies^{10, 11}) and indicate that these results are valid even at a realistic and intermediate coupling strength.

We can also specify the orbital state realized in the FM1 solution by using two angles θ_1 and θ_2 as follows,

$$\begin{aligned}
 \text{site 1; } & \cos \theta_1 |yz \rangle + \sin \theta_1 |xy \rangle, \\
 \text{site 2; } & \cos \theta_2 |zx \rangle + \sin \theta_2 |xy \rangle, \\
 \text{site 3; } & -\cos \theta_2 |yz \rangle + \sin \theta_2 |xy \rangle, \\
 \text{site 4; } & -\cos \theta_1 |zx \rangle + \sin \theta_1 |xy \rangle. \quad (22)
 \end{aligned}$$

In Fig. 7, the angles θ_1 and θ_2 are plotted as functions of the Ti-O-Ti bond angle. In the small GdFeO₃-

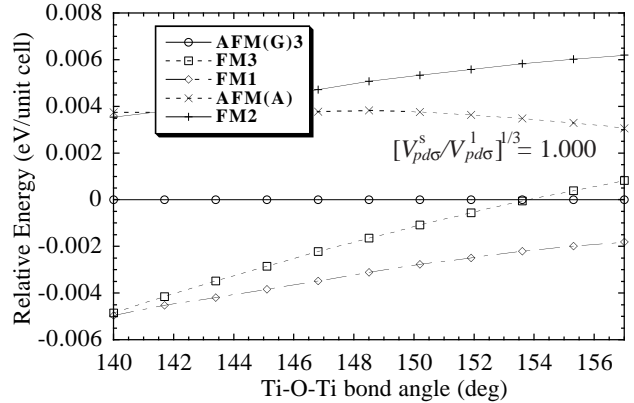


Fig. 8. Energies of various spin and orbital configurations relative to that of AFM(G)3 state as functions of the Ti-O-Ti bond angle in the case of $[V_{pd\sigma}^s/V_{pd\sigma}^l]^{1/3} = 1.000$.

type distortion ($\angle \text{Ti-O-Ti} \sim 157^\circ$), almost complete (yz, xy, xy, zx)-type occupation is realized. In this orbital ordering, the neighboring occupied-orbitals are approximately orthogonal and electron transfers from the occupied orbitals are restricted to neighboring unoccupied orbitals. However, with increasing the GdFeO₃-type distortion, the occupations of the xy, zx, yz and xy orbitals gradually increase at sites 1, 2, 3 and 4, respectively (see also Fig. 3). Therefore, both θ_1 and θ_2 tend to become close to 45° , and the orbital state in the FM1 solution become similar to that in the FM2 solution as the GdFeO₃-type distortion increases. As a result, FM1 solution in the large GdFeO₃-type distortion is similar to that of FM2 so that the energy difference between FM1 and FM2 solutions is small in the largely distorted region. This indicates that the (yz, zx, yz, zx)-type orbital ordering realized in the AFM(A) and FM2 states is strongly stabilized for the large GdFeO₃-type distortion. In addition, we note that with the large JT distortion of 1.040, the spin-orbit ground state does not have any stable solutions.

We next fix the magnitude of the JT distortion: $[V_{pd\sigma}^s/V_{pd\sigma}^l]^{1/3}$ at 1.000 (i.e. no JT distortion) in order to focus on the situation realized in LaTiO₃. In Fig. 8, relative energies of various spin and orbital configurations are plotted as functions of the Ti-O-Ti bond angle. Without the JT distortion, AFM(G)1 and AFM(G)2 states have no stable solutions.

So far, in the small GdFeO₃-type distortion, the AFM state with spin-orbit ground state [AFM(G)3], out of which two states with antiparallel spin and orbital moment, $\frac{1}{\sqrt{2}}(yz + izx) \uparrow$ and $\frac{1}{\sqrt{2}}(yz - izx) \downarrow$ are alternating between nearest neighbors, is considered to be stabilized both by the spin-orbit interaction and by the superexchange interactions. However, though this AFM(G)3 state is lower in energy relative to the FM3 state in which $\frac{1}{\sqrt{2}}(yz + izx) \uparrow$ ($\frac{1}{\sqrt{2}}(yz - izx) \downarrow$) is occupied at each site, a FM state with AF-orbital ordering (FM1) is always lower in energy as compared with AFM(G)3 and FM3 solutions. This indicates that spin-orbital superexchange interactions caused by electron transfers dominate over the couplings of the spin and orbitals due to the spin-

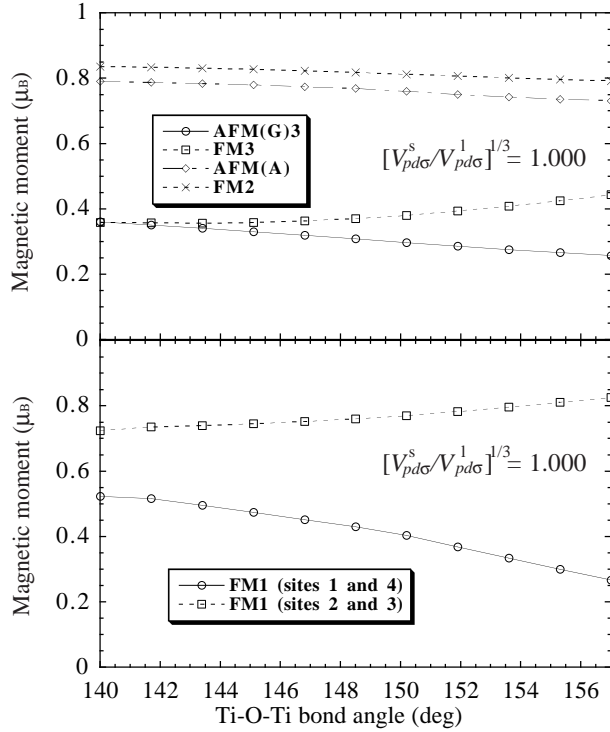


Fig. 9. Magnetic moment of various spin and orbital states as functions of the Ti-O-Ti bond angle in the case of $[V_{pd\sigma}^s/V_{pd\sigma}^l]^{1/3} = 1.000$. In the FM1 state, the magnitude of the magnetic moment is different between sites 1, 4 and sites 2, 3.

orbit interaction, and the spin-orbit interaction does not play a role in the emergence of AFM(G) state in LaTiO_3 .

In the FM1 state, the sites 1, 2, 3, and 4 are approximately occupied by $\frac{1}{\sqrt{2}}(yz + izx) \uparrow$, $xy \uparrow$, $xy \uparrow$ and $\frac{1}{\sqrt{2}}(yz + izx) \uparrow$, respectively. At sites 1 and 4, the spin-orbit ground state with antiparallel spin and orbital moment is realized. Since the neighboring $\frac{1}{\sqrt{2}}(yz + izx) \uparrow$ and xy are approximately orthogonal, AF-orbital ordering accompanied by the spin-orbit ground state is realized in FM1 solution. Consequently, this FM1 state is strongly stabilized both by the spin-orbit interaction and by the spin-orbital superexchange interactions.

In Fig. 9, the magnetic moment of various spin and orbital solutions are plotted as functions of the bond angle. In AFM(G)3 and FM3 with spin-orbit ground state, the magnetic moment is strongly reduced from the spin-only moment due to the antiparallel contribution of the unquenched orbital moment while those of AFM(A) and FM2 with JT ground state take approximately unreduced values. In FM1, reduced ordered moment is realized at sites 1 and 4 with the spin-orbit ground state while the moments are not so reduced at sites 2 and 3 in which xy orbital is dominantly occupied.

The strong stabilization of the FM1 state in the small GdFeO_3 -type distortion with no JT distortion indicates that the spin and orbital states in LaTiO_3 can not be described by the spin-orbit ground state. In addition, there exists a discrepancy between the calculated energy difference and that expected from experimentally obtained T_N of ~ 130 K. We expect the energy difference between

FM and AFM(G) solutions per unit cell from T_N in the following way. First, we can naively estimate the spin-exchange constant J in LaTiO_3 based on a comparison of T_N with the numerical study on the spin-1/2 Heisenberg model on a cubic lattice as $J = k_B T_N / 0.946 \sim 12$ meV.²⁸⁾ Then, a bond-energy difference between FM and AFM spin configurations per Ti-Ti bond is $J/2$, and there are 12 Ti-Ti bonds in the unit cell so that we can expect that AFM(G) solution is lower than FM solution in energy by $6J \sim 72$ meV within the Hartree-Fock approximation. However, this value is considerably large as compared with the characteristic order of the calculated energy difference even if the spin-orbit ground state is realized in LaTiO_3 . (For instance, the energy difference between AFM(G)3 and FM3 is ~ 1 meV per unit cell.) This discrepancy can not be explained within the error bars of the parameters estimated from the analyses of photoemission spectra so that we can conclude the spin-orbit interaction is irrelevant to the AFM(G) state in LaTiO_3 .

Here, a question arises: why is the ordered moment reduced from $1 \mu_B$ so strongly if the spin-orbit interaction can not be its origin? Recent optical measurement shows that LaTiO_3 has a considerably small optical gap of ~ 0.1 eV in the vicinity of the metal-insulator (M-I) phase boundary with strong itinerant character.⁶⁾ Therefore, in this system, we expect that some amount of charge and spin fluctuations remain. The reduction of the magnetic moment may easily be attributed to this itinerant fluctuation.²⁹⁾ For instance, in 2D case, the ordered moment $\sim 0.6 \mu_B$ for the Heisenberg model diminishes to $\leq 0.2 \mu_B$ for $U = 4$ Hubbard model due to the itinerant fluctuation accompanied by the double occupancy.²⁹⁾ This strong reduction of the ordered moment with charge fluctuations is also obtained for Hubbard model with next-nearest neighbor transfers in recent numerical study.³⁰⁾ Within the Hartree-Fock approximation, the ordered moment is equivalent to the local moment so that the reduction of the moment can not be reproduced. However, we can expect this reduction irrespective of the dimensionality in an insulator with small insulating gap near the M-I phase boundary. Consequently, though the spin moment within the spin-wave theory takes $\sim 0.844 \mu_B$ and the reduction due to the quantum effects is small in 3D spin-wave approximation, the ordered moment would easily diminishes to $\sim 0.45 \mu_B$ in LaTiO_3 with the strong itinerant character and large expectation value of the double occupancy when charge fluctuations are properly taken into account.

In Fig. 10, we show the magnetic and orbital phase diagram in the plane of the GdFeO_3 -type and d -type JT distortions. In the region of $[V_{pd\sigma}^s/V_{pd\sigma}^l]^{1/3} > 1.027$, AFM(A)-FM phase transition occurs as increasing the GdFeO_3 -type distortion. In the small GdFeO_3 -type distortion, FM state with AF-orbital ordering is stabilized in the whole range of $[V_{pd\sigma}^s/V_{pd\sigma}^l]^{1/3}$. In particular, in the small JT distortion, only FM1 state is stabilized. In FM1 state with no JT distortion, sites 1, 2, 3 and 4 are occupied by $\frac{1}{\sqrt{2}}(yz + izx) \uparrow$, $xy \uparrow$, $xy \uparrow$ and $\frac{1}{\sqrt{2}}(yz + izx) \uparrow$, respectively, and though the spin-orbit ground state is

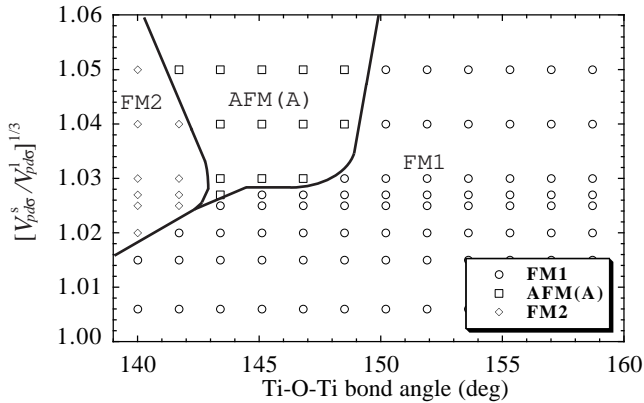


Fig. 10. Magnetic and orbital phase diagram in the plane of the GdFeO₃-type and *d*-type JT distortions.

realized at sites 1 and 4, *xy* ↑-occupancy is favored at sites 2 and 3 by the spin-orbital superexchange interactions. In addition, AFM(G) phase does not exist even for the small JT distortion.

§4. Summary and Conclusions

In this paper, we have studied the magnetic and orbital states and their phase transitions of the perovskite-type Ti oxides by using the multiband *d-p* Hamiltonian. In this Hamiltonian, effects of both electron transfers and spin-orbit interaction are considered. By applying the unrestricted Hartree-Fock approximation to this Hamiltonian, we have investigated the orbital-spin states as functions of the magnitudes of GdFeO₃-type and *d*-type JT distortions from a viewpoint of competitions of the spin-orbit interaction, JT level-splitting and spin-orbital superexchange interactions. These competitions are characteristic in *t*_{2g} systems such as titanates in contrast with *e*_g systems such as manganites since the spin-orbit interaction strongly affects the *t*_{2g} orbitals relative to the *e*_g orbitals and JT coupling is rather weak in *t*_{2g} systems while the coupling almost always dominates over the spin-orbit interaction in *e*_g systems. Our model and approach which treat the electron transfers and the spin-orbit interaction on an equal footing and in a non-perturbative manner are appropriate for the study of the competitions. We expect that the physics of AFM or AF-orbital ordering with superexchange mechanism in the strong-coupling region is connected adiabatically with the SDW-type symmetry breaking in the weak-coupling Hartree-Fock solutions. So that, we have referred the stabilization of the SDW (or orbital density wave) type solution with AFM (or AF-orbital) symmetry breaking to the superexchange mechanism.

In the perovskite-type Ti oxides, the transfers of electrons on Ti 3*d*-orbitals are governed by supertransfer processes mediated by the O 2*p* states. We can calculate the nearest-neighbor and next-nearest-neighbor *d-d* transfers (*t* and *t'*, respectively) by using perturbational expansions with respect to *d-p* and *p-p* transfers which are determined by using Slater-Koster parameters. A tight-binding (TB) Hamiltonian with thus obtained *t*

and *t'* well reproduces the band structure obtained in LDA calculations.³¹⁾ The characteristic perturbational processes for *t* and *t'* are mediated by one O ion and by two O ions, respectively. The order of *t* and *t'* are t_{pd}^2/Δ and $t_{pd}^2 t_{pp}/\Delta^2$ with *t*_{pd} and *t*_{pp} being characteristic *d-p* and *p-p* transfers, respectively. In these compounds, the order of *t*_{pp}/Δ is about ~ 0.05 at most so that *t'* is much smaller than *t*. Actually, the band structure calculated by using TB model with both *t* and *t'* is almost the same as that obtained by using the model with only *t*, particularly in the *t*_{2g}-band dispersions. When *t'* is negligible as compared with *t*, we can expect that considerable degree of nesting remains. Consequently, in these system, the Hartree-Fock calculation can give reliable results for the AFM and AF-orbital type symmetry breaking.

Similar weak coupling approach has already been applied to both end compounds LaTiO₃ and YTiO₃ by Mizokawa and Fujimori.^{8,9)} On the other hand, in this paper, the systems located near the AFM-FM phase boundary are studied by this method for the first time. Moreover, by studying a FM state with lower energy which they overlooked, we conclude that the spin-orbit interaction can not be an origin for the AFM(G) state in LaTiO₃ in contrast with their conclusion. The conclusions of this paper are as follows.

In the region of large JT distortion, the spin-orbit interaction is dominated by the JT level-splitting and the system is well described by the JT ground state. In this region, the AFM(A)-to-FM phase transition occurs with increasing the GdFeO₃-type distortion. Through this phase transition, the orbital state changes negligibly in agreement with the previous strong coupling studies.^{10,11)} The negligible change in the orbital state through this AFM(A)-FM phase transition causes a nearly continuous change in the spin-coupling along the *c*-axis, and we can attribute the strong suppressions of *T*_N and *T*_C to the resultant two-dimensionality in the spin coupling near the phase boundary. The orbital states obtained in the FM2 and AFM(A) solutions are in agreement with those obtained by the previous strong coupling approaches,^{10,11)} which indicates the validity of the results even at a realistic and intermediate coupling strength. Actually, this orbital state has already been observed in YTiO₃.²⁴⁻²⁷⁾ We expect that a similar orbital ordering may be observed in the compounds near the AFM-FM boundary such as SmTiO₃, GdTiO₃ and La_{1-y}Y_yTiO₃ (*y* ~ 0.3). Recent resonant x-ray scattering study shows that the orbital states in SmTiO₃ and GdTiO₃ have twofold symmetry similarly to YTiO₃, and this seems to be in agreement with our result.³²⁾ Here, we note that neutron scattering experiment reveals that the magnetic structure of the Ti sites in SmTiO₃ is not AFM(A) but AFM(G).³³⁾ In addition, though SmTiO₃ is located near the phase boundary, *T*_N of ~ 50 K is somewhat high relative to the previous theoretical prediction.^{10,11)} In SmTiO₃, there exist magnetic moments on the Sm sites, and Sm-Ti spin-coupling may be important for its magnetic properties while our model does not take the orbital and spin degrees of freedom on the *R* sites into account. However, our model can well de-

scribe the orbital-spin states and their phase transitions of LaTiO_3 , YTiO_3 and $\text{La}_{1-y}\text{Y}_y\text{TiO}_3$ systems with no magnetic moments on La and Y sites. Moreover, since the orbital state near the AFM-FM phase boundary is strongly stabilized irrespective of the spin structure as shown in both our weak-coupling and previous strong-coupling studies, the similar (yz, zx, yz, zx) -type orbital state is also expected to be realized in SmTiO_3 though the magnetic structure is AFM(G) due to the Sm-Ti spin-coupling.

Without a JT distortion, owing to both spin-orbit and spin-orbital superexchange interactions a FM state with the spin-orbit ground state accompanied by an AF-orbital ordering [$(\frac{1}{\sqrt{2}}(yz + izx) \uparrow, xy \uparrow, xy \uparrow, \frac{1}{\sqrt{2}}(yz + izx) \uparrow)$ -orbital ordering] is stabilized relative to the other solutions. This FM solution can not be reproduced by the previous strong coupling approach in which the spin-orbit interaction is neglected in the large JT distortion, and is studied for the first time by our weak coupling approach. In addition, AFM(G) state is higher in energy and has no stable solutions. While in this system, the spin-orbit interaction has been considered to be relevant in the small or no JT distortion so far, the spin-orbital superexchange interactions due to the electron transfers turn out to dominate over the spin-orbit interaction. Moreover, if we would take the dominance of the spin-orbit interaction, there would be a discrepancy between the calculated energy-difference and that estimated from T_N . Thus, we conclude that the spin-orbit interaction is irrelevant to the origin of AFM(G) state in LaTiO_3 , and the experimentally observed reduction of the moment can be attributed to the strong itinerant fluctuations in LaTiO_3 instead of the spin-orbit interaction. Indeed, a recent neutron-scattering experiment reveals the spin-wave spectrum of LaTiO_3 well described by a spin-1/2 isotropic Heisenberg model on the cubic lattice and the absence of unquenched orbital angular momentum.¹²⁾ This indicates that the spin-orbit interaction is not effective in this system. Our results support these experimental results and suggest another mechanism for the emergence of the AFM(G) state. We expect that effects which are not treated in our model are responsible for its origin. Recently, possible D_{3d} distortion of the TiO_6 octahedron is examined as a candidate for the origin and nature of AFM(G) state in LaTiO_3 .³⁴⁾ In this scenario, the spin-orbit interaction is dominated by the t_{2g} -level splitting due to the D_{3d} crystal field.

In addition, we have also studied a magnetic phase diagram in the plane of the GdFeO_3 -type and d -type JT distortions in order to examine how extent the physics of AFM-FM phase transition in strong coupling limit survives when the JT level-splitting competes with the spin-orbit interaction. According to the obtained phase diagram, the description of the phase transition obtained by the previous strong coupling approach is well established in the wide range of JT distortion even when the spin-orbit interaction is taken into consideration.

Acknowledgement

The author would like to thank M. Imada, T. Mizokawa, H. Asakawa, Y. Motome and N. Hamada for valuable discussions and useful comments. This work is supported by ‘‘Research for the Future Program’’ (JSPS-RFTF97P01103) from the Japan Society for the Promotion of Science.

-
- 1) For a review see M. Imada, A. Fujimori and Y. Tokura: *Rev. Mod. Phys.* **70** (1998) 1039.
 - 2) D. A. Maclean, H.-N. Ng and J. E. Greedan: *J. Solid State Chem.* **30** (1979) 35.
 - 3) J. Akimitsu *et al.*: unpublished.
 - 4) J. P. Goral, J. E. Greedan and D. A. Maclean: *J. Solid State Chem.* **43** (1982) 244.
 - 5) J. E. Greedan: *J. Less-Common Met.* **111** (1985) 335.
 - 6) Y. Okimoto, T. Katsufuji, Y. Okada, T. Arima and Y. Tokura: *Phys. Rev. B* **51** (1995) 9581.
 - 7) T. Katsufuji, Y. Taguchi and Y. Tokura: *Phys. Rev. B* **56** (1997) 10145.
 - 8) T. Mizokawa and A. Fujimori: *Phys. Rev. B* **51** (1995) 12880.
 - 9) T. Mizokawa and A. Fujimori: *Phys. Rev. B* **54** (1996) 5368.
 - 10) M. Mochizuki and M. Imada: *J. Phys. Soc. Jpn.* **69** (2000) 1982.
 - 11) M. Mochizuki and M. Imada: *J. Phys. Soc. Jpn.* **70** (2001) 1777.
 - 12) B. Keimer, D. Casa, A. Ivanov, J. W. Lynn, M. v. Zimmermann, J. P. Hill, D. Gibbs, Y. Taguchi and Y. Tokura: *Phys. Rev. Lett.* **85** (2000) 3946.
 - 13) S. Sugano, Y. Tanabe and H. Kamimura: *Multiplets of Transition Metal Ions in Crystals* (Academic, New York, 1970).
 - 14) J. C. Slater and G. F. Koster: *Phys. Rev.* **94** (1954) 1498.
 - 15) B. H. Brandow: *Adv. Phys.* **26** (1977) 651.
 - 16) J. Kanamori: *Prog. Theor. Phys.* **30** (1963) 275.
 - 17) T. Saitoh, A. E. Bocquet, T. Mizokawa and A. Fujimori: *Phys. Rev. B* **52** (1995) 7934.
 - 18) A. E. Bocquet, T. Mizokawa, K. Morikawa, A. Fujimori, S. R. Barman, K. Mati, D. D. Sarma, Y. Tokura and M. Onoda: *Phys. Rev. B* **53** (1996) 1161.
 - 19) W. A. Harrison: *Electronic Structure and the Properties of Solids* (Dover, New York, 1989).
 - 20) L. F. Mattheiss: *Phys. Rev. B* **5** (1972) 290.
 - 21) L. F. Mattheiss: *Phys. Rev. B* **6** (1972) 4718.
 - 22) H. Sawada, N. Hamada and K. Terakura: *Physica B* **237-238** (1997) 46.
 - 23) H. Sawada and K. Terakura: *Phys. Rev. B* **58** (1998) 6831.
 - 24) M. Itoh, H. Tanaka and K. Motoya: *Physica B* **237-238** (1997) 19.
 - 25) M. Itoh, M. Tsuchiya, H. Tanaka and K. Motoya: *J. Phys. Soc. Jpn.* **68** (1999) 2783.
 - 26) H. Ichikawa, J. Akimitsu, M. Nishi and K. Kakurai: *Physica B* **281-282** (2000) 482.
 - 27) J. Akimitsu, H. Ichikawa, N. Eguchi, T. Miyano, M. Nishi and K. Kakurai: *J. Phys. Soc. Jpn.* **70** (2001) 3475.
 - 28) A. W. Sandvik: *Phys. Rev. Lett.* **80** (1999) 5196.
 - 29) S. R. White, D. J. Scalapino, R. L. Sugar, E. Y. Loh, J. E. Gubernatis, R. T. Scalettar: *Phys. Rev. B* **40** (1989) 506.
 - 30) T. Kashima and M. Imada: *J. Phys. Soc. Jpn.* **70** (2001) 3052.
 - 31) N. Hamada (private communication)
 - 32) M. Kubota *et al.*: unpublished.
 - 33) G. Amow, J. E. Greedan and C. Ritter: *J. Solid State Chem.* **141** (1998) 262.
 - 34) M. Mochizuki and M. Imada: *J. Phys. Soc. Jpn.* **70** (2001) 2872.